Gasoline Effects on Spray Characteristics, Mixing and Auto-ignition Processes in a CI Engine under PPC Conditions

J. Javier López, J M. García-Oliver, A. García and V. Domenech

CMT- Motores Térmicos - Universidad Politécnica de Valencia, Camino de Vera s/n 46022 Valencia – SPAIN

(*) CORRESPONDING AUTHOR:

Dr. Antonio Garcia: angarma8@mot.upv.es

Telephone: +34 963879659

Fax: +34 963877659

Abstract

Recent research has shown that one of the paths to reduce pollutant emissions in diesel engines is to bring the operating conditions towards those of a gasoline engine, through homogeneous combustion and high octane fuels. Reduced soot, NOx, and fuel consumption are some of the benefits of using gasoline fuel combined with EGR in compression ignition engines in partially premixed combustion modes. Thus, a comparative study using diesel fuel and gasoline has been conducted focusing on the spray characteristics, mixing and autoignition process in these new combustion modes using a conventional diesel injection system.

In this work, an experimental study has been carried out comparing the effects of penetration and cone angle under non-evaporating conditions for both fuels in a constant volume test rig. Besides, liquid length measurements and combustion process under partially premixed combustion (PPC) conditions in a single cylinder transparent engine have been done. The analysis of the results for both fuels shows no major differences on penetration and spray cone angle between them. Under vaporizing conditions, diesel spray exhibited a significantly longer liquid length than gasoline, due to the higher volatility of gasoline.

In quantitative terms, liquid length was found to be 1.8 to 2.4 times longer for the diesel fuel. 1D spray model calculations confirmed the experimental results.

The combustion process evaluation under PPC conditions shows differences in ignition delay and RoHR even under same thermodynamic conditions. Besides, Combustion images indicate differences in the autoignition and combustion process for diesel and gasoline fuels. Gasoline shows lower soot radiation and better combustion phasing.

Differences in the mixing process evaluated with the 1D model show the mixing process is governed mainly by the fuel reactivity, the ignition delay and, to a lower extent, by the spray characteristics. The overall equivalence ratio obtained through the 1D model at the start of combustion is leaner for the gasoline case. This results agrees with a longer ignition delay for this fuel, due to lower fuel reactivity, and with the lower light intensity detected in the combustion images, where the leaner the equivalence ratio the lower the intensity.

Keywords: Gasoline fuel, CI engine, mixing process, autoignition, PPC combustion.

1. Introduction

Different new combustion modes have been developed in recent times with the goal of reducing pollutant emissions from the source **[1]**, thus avoiding the increasing number of expensive after-treatment systems in nowadays diesel engine powered vehicles. These new combustion modes are usually based on early injection timing strategies and on the reduction of the oxygen volume fraction using medium and high levels of exhaust gas recirculation (EGR), both strategies leading to a nearly homogeneous air-fuel mixture because of the long ignition delay decoupling the injection and combustion phases **[2]**. These approaches provide lean and low temperature combustions compared with conventional diesel engine strategies **[3].** Consequently, as different authors show in their studies **[4] [5]**, a simultaneous decrease in NOx and soot formation is achieved. Some examples of partially or fully premixed combustion are Homogeneous Charge Compression Ignition (HCCI) **[6],** Premixed Charge Compression Ignition (PCCI), Partially Premixed Combustion (PPC), Controlled Autoignition (CAI), etc.

Within this framework, high injection pressures, high swirl levels and cooled EGR are commonly used **[4]**, with the aim of delaying autoignition and reducing peak temperatures; this in turn requires higher boost pressures to achieve the required loads **[1].** Additionally, when conventional (high cetane)

diesel fuel is used in PPC combustion, important drawbacks appear related to the phasing of the heat release, which is extremely sensitive to the initial conditions of the mixture at the beginning of the compression stroke. Consequently, it is difficult to control this combustion process, which is finally limited to low loads. Therefore, by using diesel fuel under PPC mode, it is possible to obtain low NOx and low soot, but only in a narrow engine load range **[7]** and with a considerable penalty in HC and CO.

Gasoline-like fuels generally present properties of high volatility and higher resistance to auto-ignition compared with diesel fuel as presented by Kalghatgi in different studies [8] [9]. These fuels have been tested extensively focusing on performance **[9]** and emissions at high load operation **[10].** It has been demonstrated that gasoline-like fuels exhibit a long ignition delay in PPC **[10].** Gasoline-like fuels are advantageous in achieving high load conditions with very low fuel consumption and very low NOx and soot emissions **[11].**

A key factor towards the goal of using gasoline in direct injection CI engines is to characterize the fuel spray **[10] [18].** Air fuel mixing is strongly influenced by the spray behavior and fuel properties, therefore the performance and emissions of a CI engine and the requirements discussed in previous paragraphs for the PPC combustion mode depends directly on the fuel-air distribution within the mixture **[16] [17].** Several authors have evaluated the impact of gasoline on the characteristics of a diesel-like reacting spray **[7] [11]**. It is reported that a gasoline-like fuel exhibited a longer ignition delay and lift-off length compared with those of a diesel fuel. This behavior is mainly due to the differences on the fuel chemical properties. Nevertheless, the real impact of physical properties of gasoline on spray behavior, and therefore on the mixing and autoignition processes, can be still considered as a challenge, overall in transient conditions like those found in a real engine.

From the previous discussion, it can be deduced that, on the one hand, PPC using a gasoline-like fuel is a promising combustion concept to attain a clean and efficient combustion at a wider engine load range compared with diesel fuel. On the other hand, the relevant impact of the spray characteristics on the combustion behavior has also been highlighted.

Thus, the main objective of this paper is to investigate and evaluate the differences in spray characteristics and its relationship with the mixing and autoignition processes when using gasoline instead of diesel fuel in a CI engine with a common rail fuel injection system running under PPC conditions. For this purpose, the experimental spray tip penetration and the spray cone angle in non-evaporative

conditions, as well as the liquid length in evaporative non-reacting conditions have been evaluated. Additionally, the mixing process has also been quantified with a 1D model and the autoignition process was evaluated through an experimental transparent single cylinder engine. Hence, the originality of the present work is to provide a complete and exhaustive characterization from the start of injection to the combustion process by combining different experimental and modelling tools, focusing on the spray characteristics and the mixing process as well as on their relationship with the combustion process under PPC conditions, which has revealed as one of the most promising new combustion concepts.

2. Experimental setup and theoretical tools

As general methodology to better understand the effects of gasoline on the mixing and autoignition processes in PPC mode, a combination of experimental work and modeling results has been used. In this section the facilities, the characteristics of the 1D model and the data post-processing used in this study are described.

2.1 Spray characterization test rig

A non-vaporizing nitrogen test rig is used to obtain the penetration and the cone angle of the spray through optical diagnostic. The nitrogen chamber, filled with nitrogen at high pressure but at room temperature, consists of a steel cube hosting the chamber, 3 optical accesses and various connecting flanges machined into it. Figure 1 is a simple sketch of test rig. More information about the test rig is available in **[12] [13].**

Images were taken with a high speed CMOS camera Phantom V12, equipped with a 100 mm focal length ZEISS lens and with two images resolutions: one of 680 × 680 pixels and the other of 256 x 256 pixels for spray near field characterization. For the 680 x 680 resolution, 10000 fps were used, with a maximum field of view of 45 mm. For the second configuration (256 x 256 resolution) 50000 fps were used, and in this case the maximum spray visualization was 16 mm. For both cases the exposure time was 20 µs and the pixel/mm ratio was 7.92/1. The illumination used was a continuous light source. Illumination was provided by two 150 W quartz-halogen illuminators (Dolan-Jenner PL800), supplied by 8 mm optic fiber bundles positioned at 60 mm from the spray, sharply collimated and focused on the studied area, delivering an illumination of 330 W/m^2 approximately.

The images were digitally processed using the purpose-developed software CALJET **[14]**. The segmentation algorithm, based on the log-likelihood ratio test (LRT), has high accuracy in contour determination. More details about the image processing software are available in **[14] and [15].**

Table 1 shows the main characteristics of the text matrix carried out in the nitrogen test rig to evaluate the spray tip penetration and its cone angle.

2.2 Single cylinder transparent engine

Part of the experimental work was performed in a single cylinder transparent engine. The most relevant specifications of this engine are presented in Table 2.

Figure 2 shows a complete scheme of the facility, and more details about it can be found in **[12]**.

The EGR set up is a relevant system in the present engine facility. For this purpose a specific system has been used. The decrease in oxygen volume fraction of the charge was carried out by mixing nitrogen with fresh air. To achieve the desired oxygen volume fraction, a system for measuring the nitrogen mass flow rate was installed.

The experimental tests at the single cylinder engine have been conducted in skip-fire mode. At this mode only one injection event is performed every 30 cycles. This strategy is used in order to avoid temperature transients due to cycle to cycle combustion dispersion and to keep clean as long as possible the quartz window to obtain high quality images of the study. Besides, to evaluate the autoignition and mixing processes, it is very important to control the ambient conditions during the injection process event and at the start of combustion to compare cycle to cycle results.

The transparent single cylinder engine has been used to measure the experimental liquid length and to visualize the natural luminosity and the OH* radical for the operating conditions showed in Table 3.

Figure 3 shows the optical set-up and a scheme of the main characteristics of the optical engine. The optical system includes a quartz window through the piston bowl and an elliptical mirror. For liquid length measurement tests, this mirror is used to introduce light from the high power light source to the chamber to interact with the sprays to produce Mie scattering. This is a widely used optical technique for spray characterization that involves the illumination of the fuel droplets with a light source and the image of the scattered light is collected by a camera.

In the tests of combustion process characterization, radiation from the combustion process is reflected by the UV mirror towards a 50/50 beam splitter. Half of the radiation reaches the high speed camera, whereas the rest is collected into the intensified high speed camera.

The same Phantom V12 CMOS camera, equipped with a 100 mm focal length ZEISS lens is used to record both natural luminosity and liquid length images. Concerning the OH radical, the images are recorded with a high speed intensified camera Photron II with a 50 mm focal length lens and with an interferential filter at 310±5 nm. The resolution used in both cameras is 512 x 512 pixels. For phantom V12 an acquisition frequency of 12000 fps is used in order to capture the autoignition event. For the intensified high speed camera (Photron II), used to record the *OH radical, lower frequency (6000 fps) and with a constant gain for the intensifier for each fuel is used. For liquid length measurement tests 30000 fps with a resolution of 340 x 340 pixels is used to observe the first instants of the process.

2.3 Injection system and characteristics of the fuels used

The fuel injection system used in this work is based on an electronically controlled Bosch common rail. The injector mounted is a Bosch piezoelectric CRIP 3.3 equipped with a 7 holes nozzle with 154º of included angle and 97 microns of orifice diameter. Its flow capacity is 210 cm^3/30s.

Various measurements of fuel properties have been performed outside of the engine for this research work. Physical properties and energetic content have been measured following the ASTM standards and at other different temperatures, and they are summarized in Table 4. Results show that gasoline presents lower density and a great decrease in viscosity values compared with diesel fuel. It is worthy to note that 300 ppm of additive (Havoline Performance Plus) was added to improve the lubricity of the gasoline up to diesel fuel level, increasing the service life of the high pressure pump and fuel injector. The addition of the additive does not modify neither its density nor its viscosity

2.4 1D Model description (DICOM)

The data collected on the different experimental test rigs and on the single cylinder engine are used as an input for an in-house 1-D spray model, DICOM described by Desantes et al in **[16] [17]**. The main objective of using this model is to characterize the influence of injection timing, oxygen volume fraction and fuel type on the mixing process.

Physically, the model is based on the assumption that the fuel is injected with a uniform velocity at the whole nozzle section, and that momentum exchange of the fuel with the surrounding air leads to an

increase in the width of the spray as the axial distance increases. The radial growth of the spray is determined by its cone angle. The entire spray domain is divided axially in a certain number of cells that occupy the whole spray cross section.

The model solves momentum and fuel mass conservation equations for the spray. To simplify the spatial description of both properties, self-similar Gaussian profiles are assumed, which makes it possible to transform a 2D problem into a 1D one (if symmetry is assumed). The spray is discretized along its axis in dx-sized cells that occupy the whole flow cross section, and for each cell, only on-axis properties are solved. Within each cell, the amount of the fuel mass evaporated at a given time step is calculated based on the energy provided by the entrained air. In a second step, radial distribution of properties can be obtained by corresponding self-similar profiles.

On the other hand, the specific and necessary inputs for the model are the in-cylinder thermodynamical conditions (pressure, temperature and density), the spray cone angle, the fuel mass injection rate and the spray momentum. Once all this information is available, the model solves the general conservation equations for axial momentum and fuel mass in terms of the on-axis (i.e. center line) values of velocity and species mass fractions. In this research, and only for the 1D model study, the fuels used were surrogates of the real fuels: iso-octane (C_8H_{18}) as a gasoline surrogate and hexadecane ($C_{16}H_{34}$) as a diesel fuel surrogate. The agreement obtained in the following sections of both inert spray penetration and liquid length predictions compared to experiments will confirm the validity of such fuels as surrogates.

Apart from spray tip penetration and maximum liquid length, the model predictions regarding fuel mass distribution will be used. For a particular instant, a histogram of fuel mass equivalent ratio distribution will be analyzed, as shown in Figure 4. This will be used to compare the mixing process under different conditions and fuels.

3. Results and discussion

3.1 Macroscopic spray characteristics under non-vaporizing conditions

The spray penetration and the spray cone angle are presented in Figure 5 for both diesel fuel and gasoline for different injection pressures. On the one hand, a faster penetration is obtained with an increase in the injection pressure. This effect is observed for both fuels. For a given backpressure, increasing the injection pressure implies an increase in momentum flux, which ultimately results in a

higher spray velocity, and hence a faster penetration **[18]**. Besides, the diesel fuel and the gasoline spray penetration values are similar, indicating that differences in the physical fuel properties are not affecting deeply the spray penetration, at least under non-evaporative conditions. On the other hand, regarding the spray cone angle, a distinction should be made between the near zone and the stabilized zone (in this study the stabilized zone is defined once 500 μs after the start of injection are attained). Once the spray is stabilized, a similar behavior for both fuels and for different injection pressures is obtained. The value of the cone angle in the stabilized spray is about 22.7º.

Figure 6 shows results of spray penetration and cone angle for both fuels for a 650 bar constant injection pressure and two different backpressures. Spray cone angle and tip penetration are known to change with the increase of the density in the chamber. Higher density implies lower penetration and higher cone angle. It is possible to observe again how diesel fuel and gasoline present similar values when the backpressure is kept constant. In the stabilized zone, for a 55 bar backpressure the cone angle is approximately 27.4º, whereas for a lower pressure (27.5 bar) this value decreases to 22.7º. Regarding spray cone angle, differences between fuels in all the evaluated cases are lower than the experimental error of this parameter, which is near 1-1.5º for the used processing methodology. So, it is possible to conclude that no differences between spray cone angles for both fuels are observed in all the tested conditions in this work.

Thus, independently on the operation conditions tested, for any given injection pressure and chamber density, diesel fuel and gasoline are presenting similar values in terms of spray penetration and cone angle under non evaporative conditions. Considering theoretical spray penetration (S) as a function of gas density ($\boldsymbol{\rho_g}$) , momentum flux ($\boldsymbol{M_0}$) at the nozzle outlet orifice, spray cone angle ($\frac{\boldsymbol{\theta}}{\boldsymbol{2}}$) and time (t) :

$$\boldsymbol{S(t) = k \cdot \rho_g^{-1/4} \cdot M_0^{-1/4} \cdot t^{1/2} \cdot tan_0^{-\frac{1}{2}}(\frac{\theta}{2})} \qquad (1)$$

It is possible to state that results similarity between fuels is mainly due to the momentum flux in maintained constant. To clarify this behavior, it is interesting to remark that gasoline is presenting higher effective velocity compared with diesel fuel due to lower viscosity. By contrast, gasoline is presenting a lower injection rate compared with diesel fuel due to lower density **[18].** Considering momentum flux as the product of those variables, injection rate $\boldsymbol{\dot{m}_f}$ and effective velocity $\boldsymbol{U_{eff}}$, it seems that physical differences between fuels (density and viscosity) are compensated, and therefore similar momentum flux is attained between fuels **[18].**

$$M_0 = \dot{m}_f \cdot u_{eff} \quad (2)$$

To complete the previous presented experimental work and with the aim of fitting and evaluating the potential of DICOM 1-D model to predict mixing process using gasoline, some calculations have been performed. Thus, Figure 7 presents the results of the experimental spray penetration data obtained with gasoline and diesel fuel in the spray characterization test rig, together with the results of simulated spray penetration obtained with the 1-D model. To obtain these results it has been used previous experimental data from mass flow rate, momentum flux and thermodynamic conditions at spray characterization test rig. Figure 7 shows the accuracy between the results obtained with the 1-D model and the experimental data obtained. If the predicted (1-D model) and the observed (experimental) values for different injection pressures and different thermodynamic conditions are fitted, the statistic R^2 is 97.7% for gasoline and 98.4% for diesel fuel, thus proving an excellent agreement.

3.2 Spray development under vaporizing conditions

Using the single cylinder transparent engine described before and under vaporizing but non-reacting conditions, a study of liquid length has been carried out. In Figure 8, different Mie scattering images of the liquid length evolution for gasoline and diesel fuel at different instants are presented. The images presented show results from the start of injection, where the small differences in liquid length for both fuels can be observed, to the stabilized zone, where significant differences in terms of liquid length can be observed between both fuels.

The liquid length study has been divided in two steps. First, an evaluation of different start of injections, implying different in-cylinder temperatures and densities, has been carried out. Second, considering some defined in-cylinder conditions, different injection pressures have been swept.

Results for different injection timings are shown in Figure 9. In the left part of the Figure, the liquid length versus time for diesel fuel is presented, and in the right part, the same results but for gasoline are shown (to allow comparison of both Figures, each injection timing is represented by a different symbol). With gasoline fuel, the stabilized value of the liquid length is shorter than with diesel fuel. In all the evaluated cases, the value of diesel fuel liquid length is between 1.8 up to 2.4 times longer than for gasoline. To explain this behavior the research has focused on the 1-D model. Thus, a first step has consisted of evaluating the model under non reacting and evaporative conditions. Next, once the model

has been validated, a quantification of differences between fuels has been presented, considering the main variables which are governing stabilized liquid length.

In the top part of Figure 10, the experimental versus modeled transient from the start of energizing time until the stabilized conditions can be observed. For both fuels, the case with a SoI of 14 CAD bTDC has been presented. Some slight differences can be observed between the experimental results and the model predictions in the transient part of the liquid length. However, experiments and predictions show an extremely good agreement for both fuels in the stabilized zone of the liquid length.

In the bottom part of Figure 10, the simulated maximum liquid length obtained with 1-D model is compared with the experimental data at the stabilized value. Experimental and simulated results present again good agreement, with a R^2 higher than 93% for both fuels. The discrepancies that can be observed in the Figure might be derived from the experimental errors when determining the liquid length under low light intensity conditions caused by engine window and mirror fouling, which finally implies difficulties for the image processing. It is worthy to mention that in this plot all the available results are included (for different conditions, for both fuels and both experimental and modeling results). It can be observed that some groups of points appear in the plots, which correspond to different injection timings implying different maximum liquid lengths (in the stabilization region). This effect is more appreciable in the diesel fuel due to its higher values of liquid length.

Once the accuracy of 1-D model is presented, it can be stated that the maximum liquid length in steady conditions **(LL)** depends on nozzle diameter ($\boldsymbol{D_0}$), fuel density($\boldsymbol{\rho_f}$), gas density ($\boldsymbol{\rho_g}$) and vaporized fuel mass fraction ($\boldsymbol{Y_{f,evap}}$) **[19].**

$$\boldsymbol{LL = k \cdot D_0 \cdot \sqrt{\frac{\rho_f}{\rho_g}} \cdot \frac{1}{Y_{f,evap}}} \qquad (3)$$

The 1D model calculates Yfevap based on an adiabatic mixing assumption, which includes both an enthalpy balance and liquid-vapor equilibrium calculations [16]. This parameter can be considered as the fuel mass fraction where the last droplets vaporize.

Figure 11 presents the vaporized fuel mass fraction ratio between iso-octane (gasoline) and hexadecane (diesel fuel) versus different ambient temperatures maintaining constant ambient density at 25 kg/m3. Thus, keeping constant the ambient temperature, the iso-octane (gasoline) vaporized fuel mass fraction is higher than the obtained with hexadecane (diesel fuel). For this temperature sweep, the value

of the iso-octane (gasoline) vaporized fuel mass fraction is between 1.7 up to 2.3 times larger than for hexadecane (diesel fuel). Thus, it seems that the main variable which is governing the differences in terms of stabilized liquid length for both fuels is the vaporized fuel mass fraction.

Continuing with particular results showed in figure 9, it is important to point out how the ratio between diesel fuel and gasoline liquid length increases as the start of injection is advanced. This effect is mainly due to the lower chamber temperature attained when the injection timing is advanced, at least in the range used in the current research. Considering equation 3, changes on temperature will represent a great impact on vaporized fuel mass fraction and, consequently, on the liquid length **[20]** This result has been observed by other authors with test rigs in steady conditions **[21]**, but in this study it has been carried out in transient conditions (single cylinder transparent engine), and the results show similar trends.

It is important to remark that the stabilized zone for the liquid length is reached slightly earlier for the gasoline case. This behavior can be justified by two complementary explanations: on the one hand, because of the different viscosity between fuels (lower for gasoline). In fact, the early transient of the penetration curve is significantly reduced if the viscous forces are lower, since the force required to move the needle is much smaller. In this case, the injector is opened faster, and the liquid length is stabilized earlier. On the other hand, even if spray penetration were the same for both fuels, a shorter liquid length has to be obviously reached earlier since the fuel needs less time to reach the earlier stabilized liquid length position.

It is also interesting to underline that for all the tests performed with gasoline in all the SoI range tested (from -29 CAD to -14 CAD), the liquid length does not exceed 10 mm. This result is extremely relevant in the context of partially premixed combustion strategies. In fact, different studies **[22] [23]** have shown the potential of these strategies to reduce NOx and soot emissions when diesel fuel is used. However, one of their main drawbacks are HC and CO emissions, both partially related to the wall impingement of the liquid fuel due to the significantly advanced SoI used in these strategies together with the use of diesel fuel. Based on the previous results, the use of gasoline instead of diesel fuel could reduce this problem extensively.

In Figure 12, liquid length results for both fuels and for different injection pressures (650, 1050 and 1450 bar) are shown. In this case all the tests were carried out keeping constant the in-cylinder chamber conditions. No differences in terms of stabilized liquid length can be appreciated for the

different injection pressures for a given fuel. Considering equation (3) this behavior is completely expected. However, when the results obtained for each fuel are compared, a liquid length about 2 times longer for the diesel fuel can be found at these conditions. It is worth to mention that these tests have been carried out near top dead center (5 CAD bTDC, i.e. 1200 μs before TDC) where ambient density and ambient temperature are maximum.

3.3 Mixing and combustion process evaluation under partially premixed conditions

Once the inert spray analysis has been presented, partially premixed combustion results for both fuels, using a transparent single cylinder engine, will be presented in the current section. Together with the results of the combustion process, some information coming from a computational study of the mixing process using the experimental ignition delay and the 1D model will be given so as to further analyze the results.

Figure 13 shows the experimental results obtained with the combustion diagnosis and processed images. On the top of the Figure, the integrated natural luminosity (Icummul) is plotted as obtained from the natural luminosity images. Below, the injected mass flow rate and the rate of heat release have been plotted. Finally, at the bottom of the Figure, some images representative of the main instants of the PPC process (natural luminosity and OH* radical) are presented.

The test presented in Figure 13 has been conducted under the same thermodynamic conditions for both diesel fuel and gasoline. To achieve similar IMEP conditions for both fuels, a lower oxygen volume fraction has been used (O_2 =12%) in the diesel fuel case. Even in this scenario, it can be observed how the diesel fuel combustion process starts much earlier than that with gasoline the RoHR of diesel fuel starts at 8.5 CAD bTDC, whereas it starts at 0.5 CAD bTDC for the gasoline case. This higher extra mixing time is mainly controlled by chemical kinetics and represents the highest difference in the mixing process between the two cases. Some other differences between diesel fuel and gasoline profiles can be observed. For instance, for the gasoline case, there is not a clear bump of cool flames in the RoHR as in the diesel fuel case: this is mainly due to the chemical mechanism that promotes cool flames, which does not exist in the gasoline molecular structure **[24]**. Additionally the RoHR profile has a higher peak value for the gasoline case, as well as a slightly lower combustion duration.

Thanks to the natural luminosity images it is possible to observe how higher luminosity is observed in the combustion chamber for the diesel fuel case presenting a higher integrated natural luminosity. A red zone (tracer of high intensity) in the image taken at 3.40 CAD bTDC can be clearly observed for the diesel fuel case. This zone does not appear for the gasoline case, mainly due to the higher homogeneity and lower equivalence ratios during the combustion process. Based on the OH* radical luminosity images, it can be said that lower homogeneity exists for the diesel fuel case for all the time steps evaluated.

To provide more detail and show differences in local conditions attained at start of combustion, figure 14 (left) shows the mass distribution under different equivalence ratios for both fuels at the experimental start of combustion instant. It is important to note how in this case, because of the differences in chemical kinetics leading to differences in ignition timing ($SoC_{Gasoline}$ = 0.5 CAD bTDC and SoC_{diesel}=8.5 CADbTDC), the distribution for both fuels changes, being more homogeneous and clearly leaner for gasoline. The maximal local equivalence ratio for iso-octacne (gasoline) is almost the stoichiometric, by contrast for hexadecane (diesel fuel) is around the double. For some given thermodynamic conditions, this extra mixing time is mainly controlled by the differences in fuel reactivity. It is necessary to point out that even if a lower air reactivity (O_2 volume fraction of 12%) is used for the diesel fuel case, the extra mixing time remains shorter than gasoline, thus leading to differences in the mixing process. Finally, this involves leaner mixtures and promotes a more homogenous combustion for the gasoline case. This result can be appreciated through the lower luminosity observable at the cumulative intensity in Figure 13, where the values for the diesel fuel case are one order of magnitude above those corresponding to gasoline. Moreover, a higher homogeneity and a lower intensity can be observed for the gasoline case, both for natural luminosity and *OH radical images. To comprehend in more detail the differences in mixing process when gasoline and diesel fuel are used and with the aim of avoiding chemical effects on this process, figure 14 (right) presents the mass distribution under different equivalence ratios for both fuels at the same start of combustion (0.5 ms after the EoI). Experimentally, this approach could be get using a higher amount of EGR for the diesel case. Nevertheless, it is interesting to remark that this is only a theoretical approach. Thus, considering only physical differences between iso-octane (gasoline) and hexadecane (diesel fuel), neither difference in mixing process is attained. Therefore, it is demonstrated that different fuel reactivity is governing differences in mixing process.

4. Conclusions

In this study, an experimental and theoretical study has been carried out to explore the mixing and the autoignition processes in PPC combustion mode conditions with two different fuels with different reactivity and physical characteristics: diesel fuel and gasoline. The main conclusions of the work are addressed as follows:

- Under non-evaporating conditions, gasoline and diesel fuel do have a similar spray behavior. Both spray penetration and spray cone angle for all the parametric studies performed showed similar trends and values. Therefore, mixing processes under these conditions, non-evaporative and non-reactive, are practically the same for gasoline and for diesel fuel, and this is confirmed because the momentum flux results are very similar for both fuels.

- The experimental liquid length studies showed that gasoline has shorter liquid length than diesel fuel for all the evaluated ranges under transient conditions. These differences have been quantified experimental and numerically. The vaporized fuel mass fraction was found to be the key parameter governing these differences for both fuels under stabilized conditions.

- Even if less reactivity conditions are considered for the diesel fuel case, lower intake oxygen volume fraction, the gasoline case presents a higher extra mixing time. Hence, for this latter case, there is an increased time to further mix fuel and air, leading to a leaner and more homogeneous mixture. In particular, local richer equivalences ratios are attained with diesel fuel compared with gasoline due to delayed gasoline start of combustion. This behavior is consistent with higher light intensity showed for diesel fuel images taken during a PPC combustion process

- In terms of differences on mixing process under evaporative and reacting conditions due to the use of diesel or gasoline fuel, it is possible to state that avoiding chemical reactivity differences, both fuels would present the same mixture distribution. Nevertheless, considering real differences in the start of combustion due to different kinetics, completely leaner mixing process is attained for gasoline. Thus, physical differences between fuels are not implying differences on mixing process.

References

[1] Yang, J., Culp, T., and Kenney, T. Development of a gasoline engine system using HCCI technology- The concept and the test results. SAE paper 2002-1-2832.

[2] Musculus, M.P.B., Miles, P.C., Pickett, L.M. "Conceptual model for partially premixed Diesel combustion". Progress in Energy and Combustion science, Volume 39, pp. 246-283, 2013.

[3] Hanson, R. M., Kokjohn, S. L., Splitter, D. A, and Reitz, R. D. "An experimental Investigation of Fuel Reactivity Controlled PCCI Combustion in a Heavy-Duty Engine" SAE international journal of engines, 2010, 3(1) 700-716.

[4] Benajes, J., Novella, R., Garcia, A., Domenech, V. "An investigation on mixing and autoignition using Diesel and gasoline in a direct injection compression ignition engine operating in PCCI combustion conditions". SAE Int. J. Engines, Volume 4, pp. 2590-2602, 2011.

[5] Keeler, B., Shayler, P.J. "Constraints on Fuel Injection and EGR Strategies for Diesel PCCI-Type Combustion". SAE 2008-01-1327.

[6] Mingfa, Y., Zhaolei, Z., Haifeng, L. "Progress and recent trends in homogeneous charge compression ignition (HCCI) engines". Progress in Energy and Combustion Science, Volume 35, Issue 5, October 2009, Pages 398-437.

[7] Johansson, B. "Path to High Efficiency Gasoline Engine". DEER 2010 Lund University.

[8] Kalghatgi, G.T., Risberg, P., and Ångström, H.-E., "Advantages of Fuels with High Resistance to Auto-Ignition in Late-Injection, Low-Temperature, Compression Ignition Combustion," SAE Technical Paper 2006-01-3385, 2006.

[9] Kalghatgi, G.T., Risberg, P., and Ångström, H.-E., "Partially Pre-Mixed Auto-Ignition of Gasoline to Attain Low Smoke and Low NOx at High Load in a Compression Ignition Engine and Comparison with a Diesel Fuel," SAE Technical Paper 2007-01-0006, 2007.

[10] Kim, K., Kim, D., Jung, Y., Bae, C. "Spray and combustion characteristic of gasoline and Diesel in a direct injection compression ignition engine". Fuel, Volume 109, pp. 616-626, 2013.

[11] Hildingsson, L., Kalghatgi, G., Tait, N., Johansson, B. et al., "Fuel Octane Effects in the Partially Premixed Combustion Regime in Compression Ignition Engines," SAE Technical Paper 2009-01-2648, 2009.

[12] Pastor, J.V., García-Oliver, J.M., Pastor JM, Ramírez-Hernández, J.G. "Experimental facility and methodology for systematic studies of cold startability in direct injection Diesel engines". Measurement Science and Technology, Volume 20 pp.95-109, 2011.

[13] Desantes, J.M., Payri, R., Salvador, F.J., Soare, V. "Determination of Diesel sprays characteristics in real engine in-cylinder air density and pressure conditions". Mech. Sci. Technology, Volume 19, pp. 2040–2052, 2005.

[14] Pastor, J.V., Arregle, J., Palomares, A. "Diesel spray image segmentation with a likelihood ratio test". Appl. Opt. 2001, Volume 40, (No. 17), pp. 2876–2885, 2001.

[15] Macian, V., Payri, R., Garcia, A., Bardi, M. "Experimental Evaluation of the Best Approach for Diesel Spray Images Segmentation", Experimental Technique, Volume 36, Issue 6, pp.26-34, 2012.

[16] Pastor J.V., Lopez J.J., Garcia J. M., Pastor J. M. "A 1D model for the description of mixing-controlled inert Diesel sprays". Fuel, Volume 87 no.13-14, pp. 2871-2885, 2008.

[17] Desantes, J.M., Pastor, J.V., García-Oliver, J.M., Pastor, J.M. "A 1D model for the description of mixing-controlled reacting Diesel sprays", Combustion and Flame, Volume 156, pp. 234-249, 2009.

[18] Payri, R., García, A., Domenech, V., Durrett, R., Plazas, A H. An experimental study of gasoline effects on injection rate, momentum flux and spray characteristics using a common rail Diesel injection system. Fuel, Volume 97, pp. 390-399, 2012.

[19] Desantes, J.M, Pastor, J.V., Payri, R., Pastor, J.M. "Experimental characterization of internal nozzle flow and Diesel spray behavior. Part II: evaporative conditions." Atomization and Spray, Volume 22, Issue 15, pp. 517-544, 2005.

[20] Mounaim-Roussele, C., Dernotte, J., Foucher, F., Hespel, C., Houille, S. "Influence of fuel properties on the spray development characteristics in a Diesel optical access engine". In: 10th International Symposium on Combustion diagnosis. pp. 243-249, 2012.

[21] Kay, P.J., Bowen, P.J., Gold, M., Sapsford, S.M. "Studies of Gasoline Direct-injection sprays at elevated ambient gas temperature and pressures". Atomization and Spray, Volume 22, Issue 4, pp. 305-331, 2012.

[22] Torregrosa, A.J., Broatch, A., García, A., Mónico, L.F. "Sensitivity of combustion noise and NOx and soot emissions to pilot injection in PCCI Diesel engines". Applied Energy Volume 104, April 2013, pp.149-157.

[23] Ma, S., Zheng, Z., Liu, H., Zhang, Q., Yao, M. "Experimental investigation of the effects of diesel injection strategy on gasoline/diesel dual-fuel combustion". Applied Energy Volume 109, September 2013, pp. 202–212

[24] Curran, H. J., P. Gaffuri, W. J. Pitz, and C. K. Westbrook, "A Comprehensive Modeling Study of n-Heptane Oxidation". Combustion and Flame 1998, Volume 114, pp. 149-177 (1998).

ABREVIATIONS

bTDC: Crankshaft angle degrees before top dead center

aTDC: Crankshaft angle degrees after top dead center

XO_2: Oxygen volume fraction

EGR: Exhaust Gas Recirculation

EMT: Extra Mixing Time

EoI: End of Injection

EoC: End of Combustion

HC: Unburned hydrocarbons

HCCI: Homogeneous Charge Compression Ignition

RoHR: Rate of Heat Release

IMEP: Indicated Mean Effective Pressure

LL: Liquid length

LTC: Low Temperature Combustion

NO_x: Nitrogen oxides

PCCI: Premixed Charge Compression Ignition

PPC: Partially Premixed Combustion

PM: Particulate Matter

RoHR: Rate of Heat Release

SoI: Start of Injection

SoC: Start of combustion

SoE: Start of energizing time

TDC: Top Dead Center

Φ: Equivalence ratio

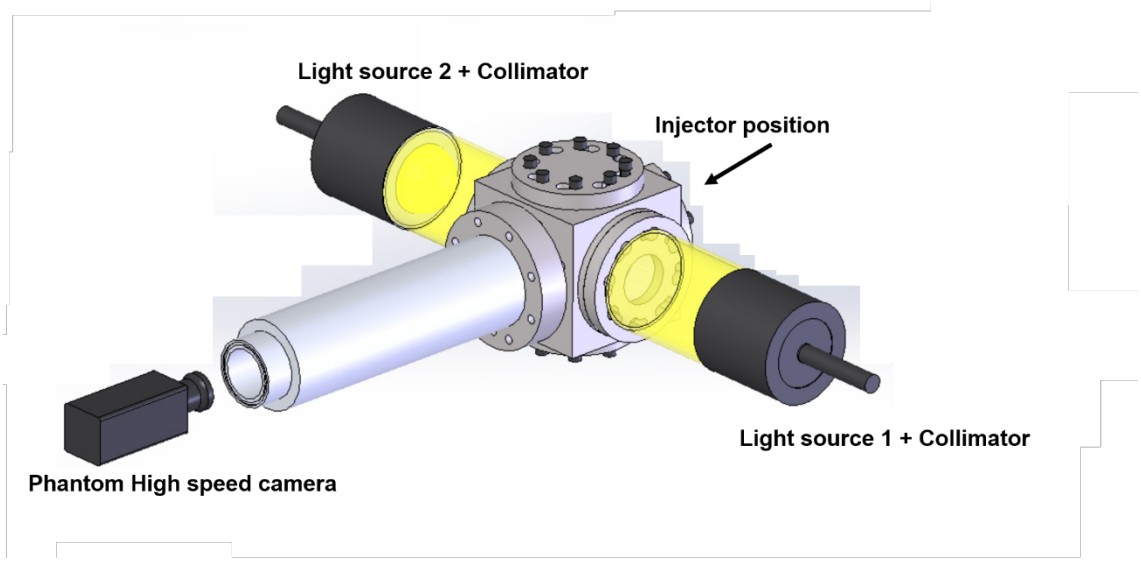

Figure 1: Optical set-up for spray characterization

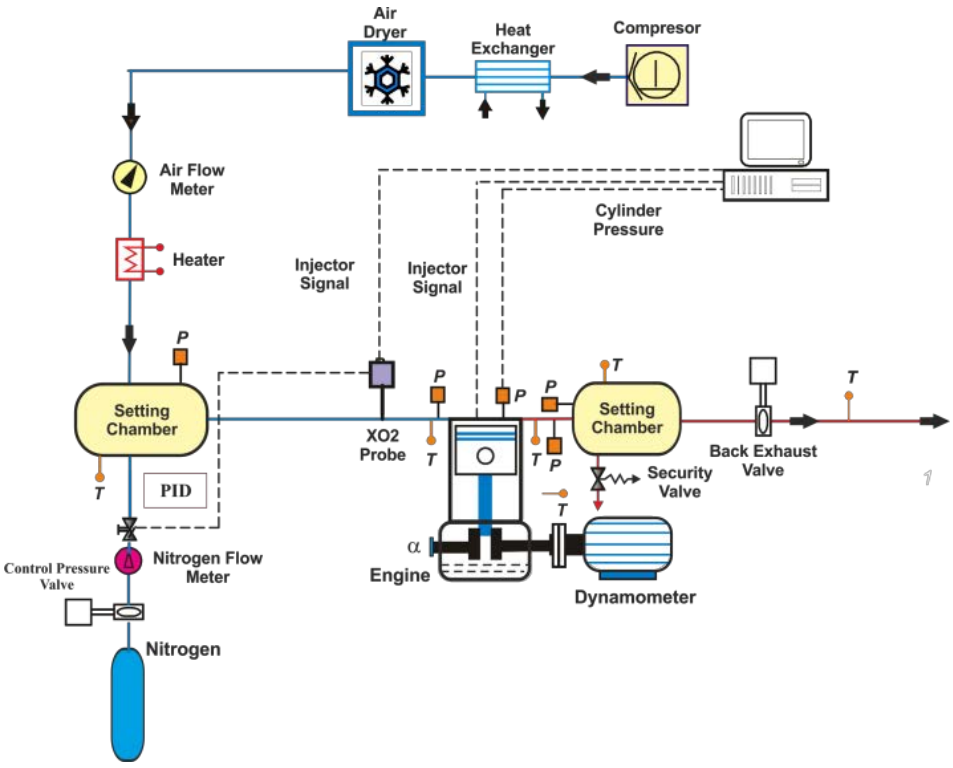

Figure 2: Complete test cell scheme

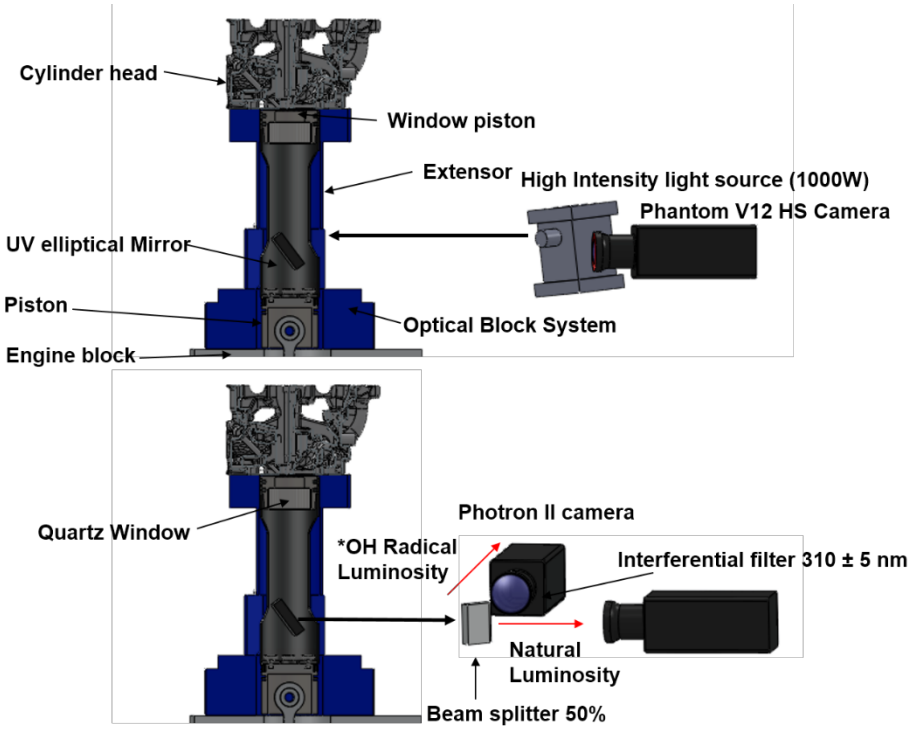

Figure 3: Scheme section of optical engine and characteristics. (A) Optical set-up for liquid length measurements. (B) Optical set-up for natural luminosity and OH* radical visualization.

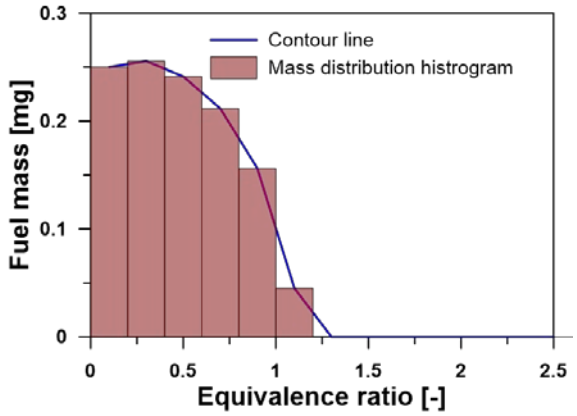

Figure 4: 1D Model pot process to obtain mass distribution under different equivalence ratio for selected instant step of the calculation

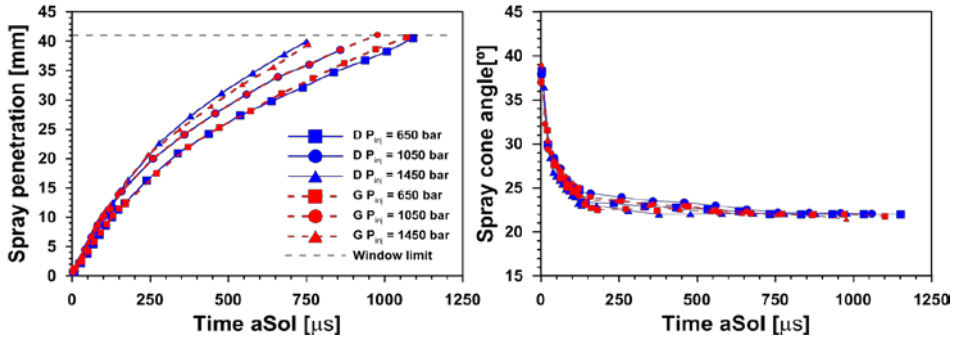

Figure 5: Spray tip penetration and cone angle for different injection pressures (650, 1050 and 1450 bar) and both fuels keeping constant density 27.5 kg/m3.

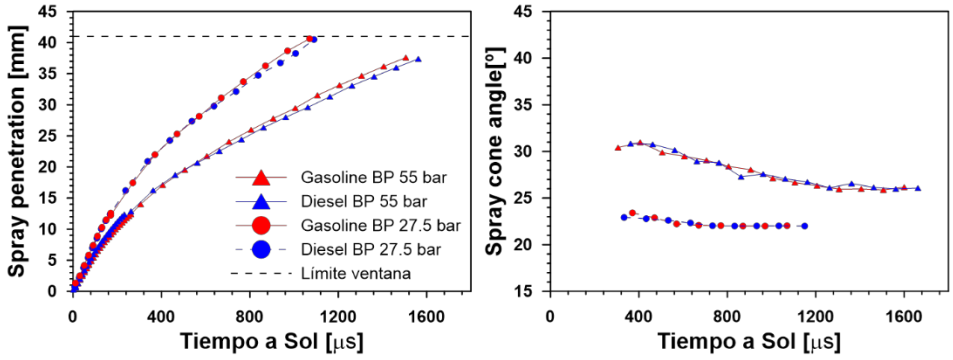

Figure 6: Spray tip penetration and cone angle for two different backpressure (27.5 and 55 bar) for a 650 bar injection pressure.

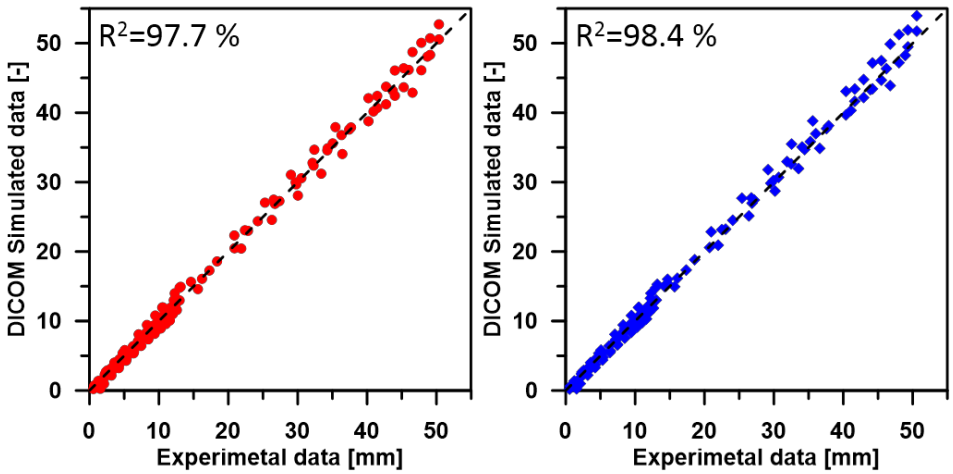

Figure 7: Experimental penetration with Diesel and gasoline versus DICOM simulated.

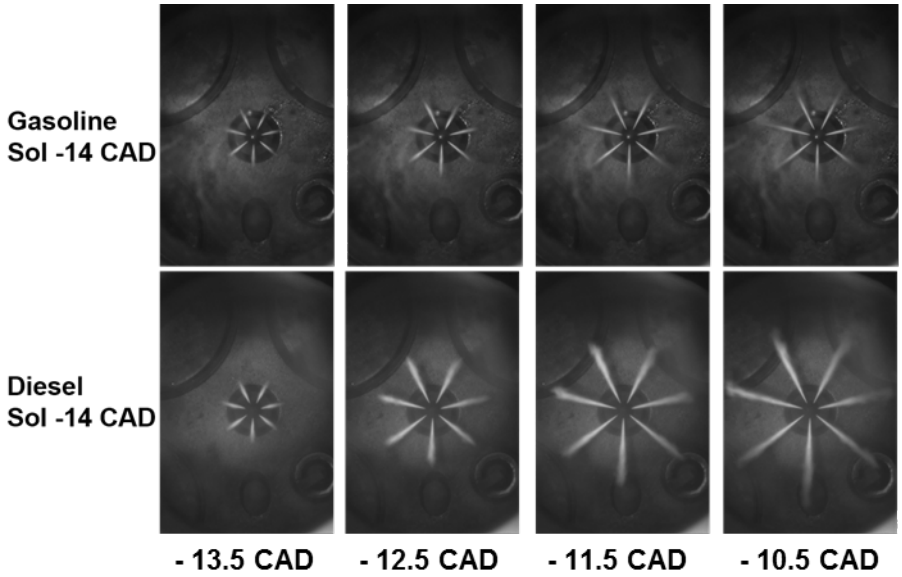

Figure 8: Temporal evolution images of liquid length for Diesel and gasoline

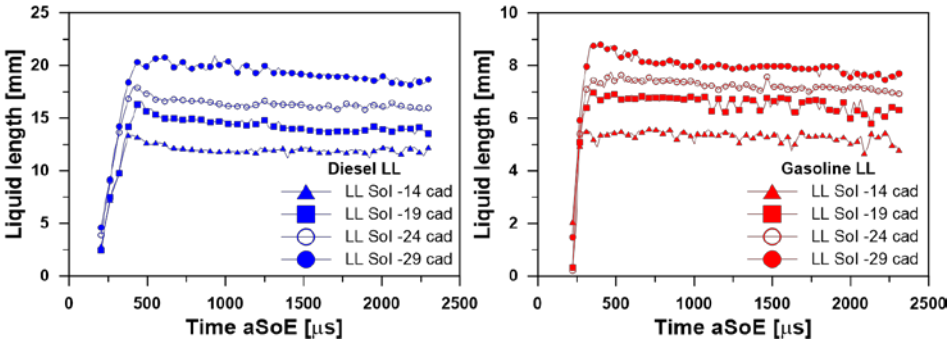

Figure 9: Liquid length for different density and temperature. (different start of injection -14, -19, -24 and -29 CAD)

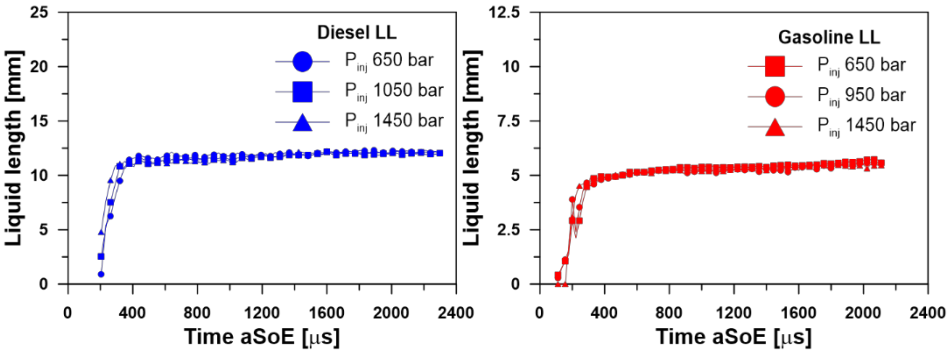

Figure 10: Liquid length for different injection pressures (650, 1050 and 1450 bar) and both fuel.

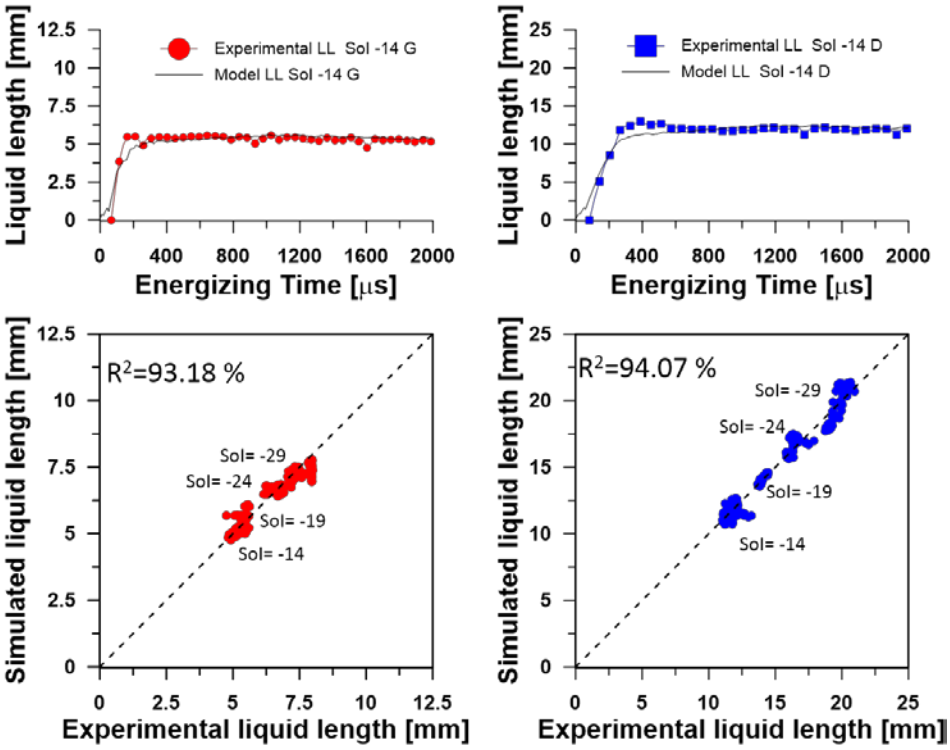

Figure 11: Experimental and simulated liquid length versus time for diesel and gasoline fuel (SoI -14 CAD). Simulated maximum liquid length versus experimental maximum liquid length for both fuels.

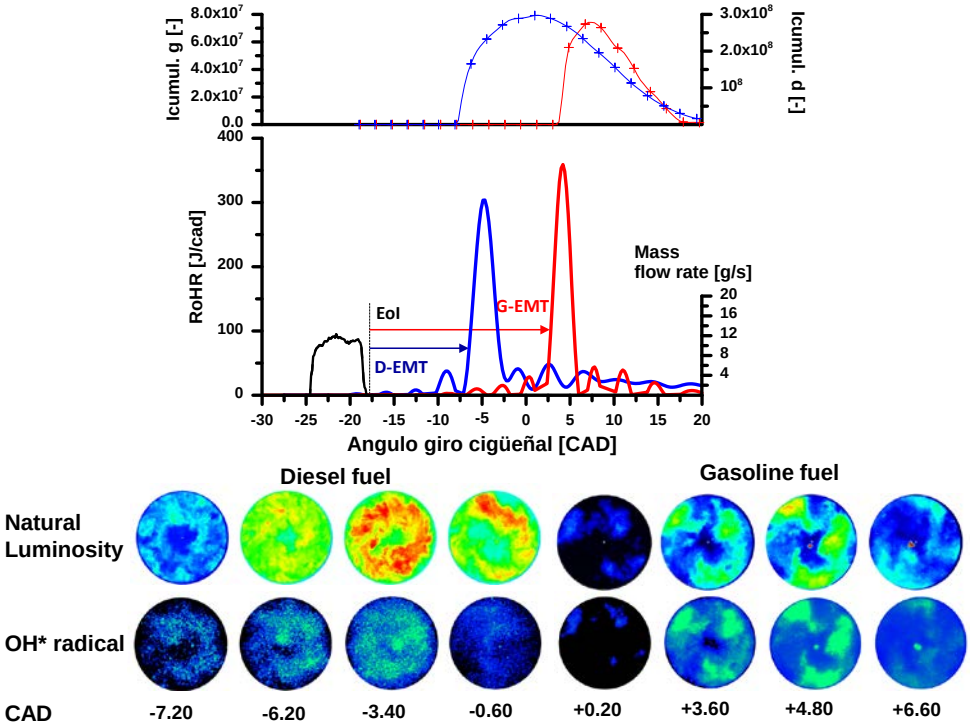

Figure 12: Partially premixed combustion process under similar IMEP values for Diesel and gasoline. Signals derived from the pressure signal and images of natural light and the OH radical and for both fuels.

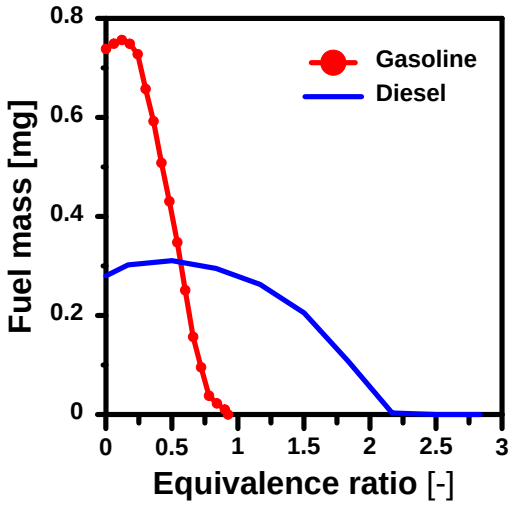

Figure 13: Fuel mass distribution under equivalence ratio at SoC time for both fuels. Time calculation derived from experimental extra mixing time.